Acta Mechanica Slovaca 13 (3): 84-95, 2009
DOI: 10.2478/v10147-010-0050-0

Properties and Performance of Hard Coatings on Tool Steels under Cyclic Indentation

ALINA SIVITSKI (EE) alina.sivitski@ttu.ee
ANDRE GREGOR (EE) andre.gregor@ttu.ee
MART SAARNA (EE) saarna@staff.ttu.ee
PRIIT KULU (EE) priit.kulu@ttu.ee
FJODOR SERGEJEV (EE) fjodor.sergejev@ttu.ee

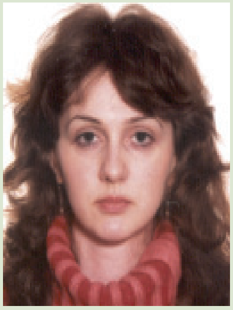

ABSTRACT
In this paper cracking resistance and fatigue properties of five hard coatings - TiN, TiCN, TiAlN, AlTiN and nanocomposite nACo® ($nc - AlTiN/a - Si_3N_4$) on tool steels - Weartec™ and Vanadis 6 are evaluated by means of the cyclic Vickers indentation method. The analytical part covers an evaluation of damage evolution of the coated system versus the number of cycles. The effect of mechanical response - Young's module/Hardness ratio (E/H ratio) on the crack propagation is described in the form of a diagram with various curves, each one associated with a certain number of indentation cycles. The comparative adhesion testing was conducted with the use of the Rockwell C technique. It was found that the type of cracks formed in the coated systems under cyclic loading is dependant on the E/H ratio values. The data obtained enable the cracking and fatigue resistance of the coated system to be compared and an optimal coating for metal forming tools applications to be selected.

KEYWORDS
PVD, hard coating, multilayers, indentation method, cracking, delamination.

INTRODUCTION
Knowledge of functional properties of hard coatings has gained increasing importance as the application of PVD coatings for sheet metal cold forming and cutting tools has grown recently. Fatigue and cracking resistance are the most important properties in such long-term applications where the alternating loads are applied. Investigations of coating crack development intensity and fatigue are commonly carried out using an indentation method for its ability of measuring mechanical properties in a microscopic range [11, 14, 8].

There is a lack of generality in indentation-cracking behaviour for coated systems in publications. Most of available published works [11, 16] on the cracking resistance of hard coatings explain the morphology of a film crack under static indentation, although cyclic indentation gives more precise estimates for long-term damage mechanisms. The papers on cyclic indentation of hard films investigate contact fatigue with the use of spherical [14] or conical indenters. However, Vickers pyramid indentation has an advantage over spherical and conical ones. A far more accurate measurement of the length of radial crack propagating from square indentation imprint corners can be obtained as compared to the circle impression. As hard coatings are brittle films, there is some interest in publications which focus on indentation cracking [4, 8] and fatigue [8, 12, 6] of brittle materials.

The main elements of damage evolution and fatigue response in coated brittle systems are mechanical properties, microstructure and deposition technique. Previous research

[4, 2, 3] shows that cracking resistance and cracks types of ceramics are strongly dependant on the values of Young's module/Hardness ratio (E/H ratio). Another aspect that has an effect on coated system cracking and fatigue is the substrate material and its microstructure. Different crystal structures of the substrate and the coating can cause poor adhesion between them. Additionally, cyclic indentation tests on ceramics reveal that fine and homogeneous material structures are preferable as they are characterized by slow crack growth [8].

In single loading experiments, it is required to determine deformation models of a coated system. Three types of deformation models were observed during the single indentation cycle in previous research [11]: 1 - elastic deformation of the coating and plastic deformation of the substrate without cracking (plastic zone model), 2 - cracking of the layer directly beneath the indenter (contact region model) and 3 - cracking of the layer beneath the indenter and the uplift of the substrate near the indenter causing elastic bending of the coating (uplift model). However, under cyclic indentation, elastic brittle hard coatings do not show plastic deformation up to tensile fracture (normal stress) and may not suffer fatigue damage and the fracture criterion obeys static strength. Thus, the propagation of the crack of the coated system may be attributed to the ratcheting deformation of the substrate under cyclic indentation.

In order to determine the damage mode of a coated system, crack types are determined. Five major crack types are observed in brittle materials during single indentation tests [4, 8]: cone, radial, median, half-penny, and lateral (circumferential) cracks. Previous observations [8, 9, 13] of mechanical sectioning of brittle materials indentation tests revealed that the cracks emanating from the corners of indent impressions are mostly radials cracks (Palmqvist cracks). After the crack type determination, the contact damage models in cyclic loading for brittle materials are described [8]. The tensile-driven cone cracking ("brittle" mode) and shear-driven microdamage accumulation ("quasi-plastic" mode) were determined [8].

This paper investigates cracking resistance of hard ceramics coatings subjected to cyclic Vickers indentation. Crack types and the intensity of the dependence of crack development on the coating type, deposition parameters and substrate material by analogy with Richter [8] are determined. To compare the results from different testing procedures adhesion testing is performed using Rockwell C apparatus.

EXPERIMENTAL PROCEDURE

MATERIALS

A chromium-molybdenum-vanadium alloyed spray formed (SF) cold work tool steel - Weartec^{TM} and powder metallurgical (PM) high-speed steel (HSS) - Vanadis 6 produced by Uddeholm are used as substrates for coating deposition. Chemical compositions and hardness of tool steels are listed in Table 1.

According to the manufacturer, high carbide content, size and distribution of carbides of the studied tool steels gives them an excellent friction wear (Weartec^{TM}) and chipping/cracking resistance (Vanadis 6). Powder steels, such as Vanadis 6 (Fig. 1 (b)), have smaller carbide size than spray formed steels. Smaller grain size and carbides give a more uniform structure resulting in more homogenous PM steel and better fracture and fatigue properties.

Five different PVD coatings, among them monolayer TiN and multilayer gradient TiCN, nanocomposite coating nACo® ($nc-AlTiN/a-Si_3N_4$), TiAlN and AlTiN were studied in this work. TiAlN and AlTiN coatings were deposited only on Weartec^{TM} substrate in order to reduce the number of experiments. Mechanical properties of the coatings (Table 2) were obtained by MTS Nano Indenter XP®. The nanoindentation was performed in a depth mode, a target depth of 150 nm and average indentation force of 12 mN were applied. The thickness of the coatings measured by Kalotester kaloMax® was about 2.3 μm.

The results presented in Table 2 are in good correlation with those available in the literature. In [7] the TiN coating with a thickness of 2.1 μm on HSS Bhler S790 ISOMATRIX had the nanohardness of 27 GPa and Young's modulus about 305 GPa. Fouvry et al. [5] investigated a TiCN coating with a thickness of 2.5 μm on HSS Vanadis 23 (Young's modulus of 230 GPa), which had Young's modulus of 550 GPa.

Table 1: *Chemical compositions, mechanical and surface properties of substrate materials.*

Substrate	Chemical composition, wt%						Hardness HRC / HV30	Young's modulus E (GPa)	Surface roughness Ra (μm)
	C	Si	Mn	Cr	Mo	V			
Weartec^{TM}	2.8	0.8	0.7	7.0	2.3	8.9	64 / 843	199	0.51±0.10
Vanadis 6	2.1	1.0	0.4	6.8	1.5	5.4	64 / 843	210	0.51±0.10

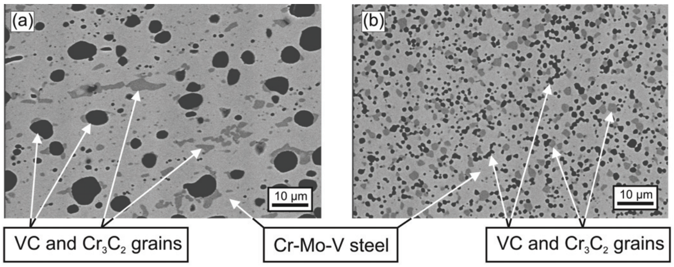

Fig. 1: *SEM micrographs of steels microstructures: (a) Weartec^{TM} (SF) and (b) Vanadis 6 (PM).*

Cross-sections of PVD coated specimens observed on the scanning electron microscope (SEM) are presented in Fig. 2.

The substrate materials and coating surface roughness were measured by a surface roughness measuring instrument of Taylor Hobson Ltd. Surtronic 3+ (using CR filter) with an accuracy of 2% (Tables1 and 2). For the substrate material, the surface roughness (R_a) was equal to 0.51 μm on the evaluation length of 4.0 mm.

COATING DEPOSITION PROCEDURE

Samples (plates) with sizes of 20x20x5 mm of two different substrate materials (Weartec^{TM} and Vanadis 6) were prepared for the deposition of PVD hard coatings and heat treated to a fixed hardness value (Table 1).

After grinding and diamond polishing (powder grain size 1 μm) all samples were degreased ultrasonically in the phosphate-alkali solution, rinsed in ethanol and dried in air. Coatings were deposited using an arc ion plating PVD technique, on π-80 Platit equipment. The parameters of the deposition process varied from coating to coating and are presented in Table 3 with reference to the coating.

CYCLIC INDENTATION TEST PROCEDURE

A servo hydraulic fatigue test system INSTRON 8800 and Vickers diamond pyramid indenter were used in the indentation experiments. The number of cycles varied from 1 up to 10 000 and a total indenting load of 500 N was applied. The application of a high indenting force is based on the results of previous studies. The application of a high indenting force is based on the results of previous study [11]. Indentation testing was carried out in the load control mode with a mean compressive load level of 275 N, alternating load of 225 N and stress ratio R = 0.1 using a sinusoidal loading pattern. The loading frequency varied from 0.5 up to 15 Hz within 1 to 1000 and 10 000 cycles, respectively.

The Palmqvist method [10] was applied for coated samples to evaluate radial cracks, based on the length measurements of the cracks emanating from the indentation impression corners. The optical microscope Axiovert 25 (ZEISS) with 500x magnification along with Buehler Omnimet Image Analysis System 5.40 with the package for image

Table 2: *Mechanical and surface properties of coatings.*

Coating/ Substrate	**Type**	**Young's modulus E (GPa)**	**Nanohardness (GPa)**	**E/H ratio**	**Surface roughness R_a (μm)**
TiN	Monolayer	438±80	28.5±0.6	15.4	0.08±0.01
TiCN	Multilayer	500±90	26.6±1.4	18.8	0.10±0.04
nACo®	Nanocomposite	323±13	29.0±1.5	11.1	0.10±0.04
TiAlN	Multilayer	301±90	19.9±1.2	15.2	0.10±0.04
AlTiN	Multilayer	336±13	23.8±1.0	14.1	0.05±0.01

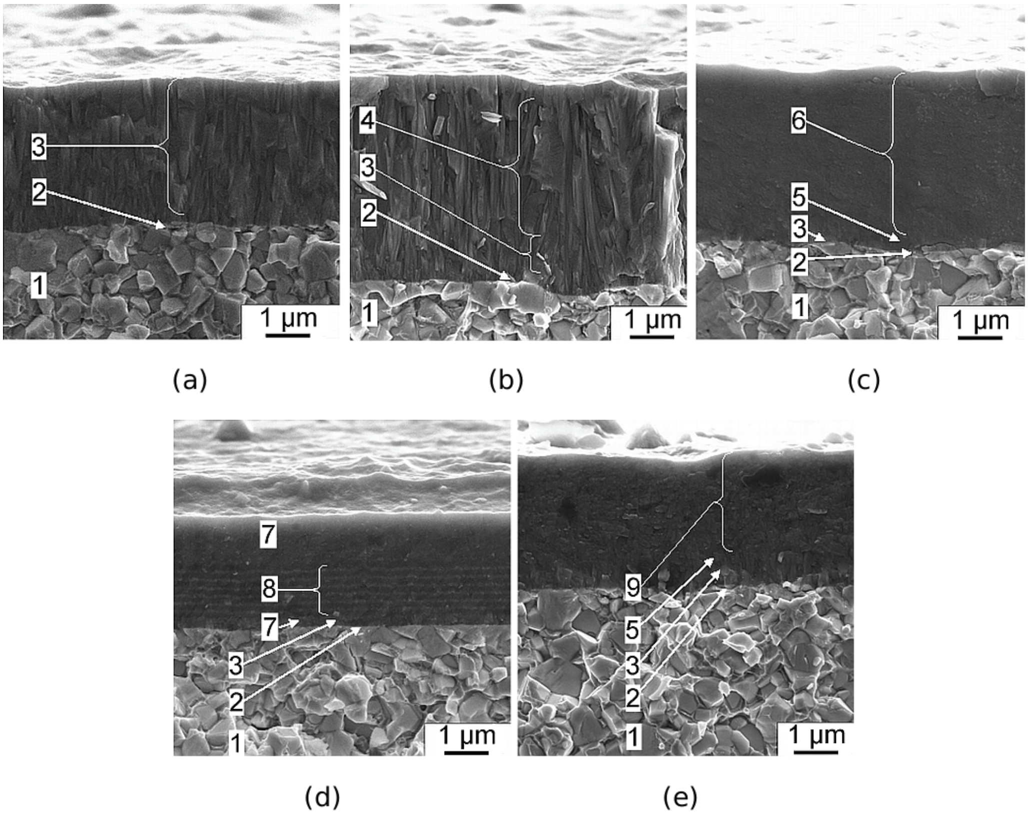

Fig. 2: *SEM images of fractured surface of hard PVD coatings: (a) TiN; (b) TiCN; (c) nACo;(d) TiAlN; (e) AlTiN. 1- substrate; 2 - Ti adhesion layer; 3 - TiN layer; 4 - TiCN gradient coating; 5 - TiAlN gradient layer + AlTiN gradient layer; 6 -* nc – AlTiN/a – Si_3N_4 *gradient coating; 7 - TiAlN layer; 8 - TiAlN/AlN multilayer coating; 9 - AlTiN gradient coating.*

Table 3: *Deposition parameters.*

Coating	Bias voltage (V)	Pressure (mbar)	Ti - Al / AlSi cathode arc current (A)	Temp. (°C)	Ar flow (sccm)	N_2 flow (sccm)	C_2H_2 flow (sccm)
TiN	-75 ... -120	8×10^{-3}	100 ... 125/-	450	6	200	–
TiCN	-60 ... -120	$(5\ldots7) \times 10^{-3}$	120 ... 130/-	450	6	165 ... 180	7...39
nACo	-75 ... -150	$9 \times 10^{-3} \ldots 1.2 \times 10^{-2}$	82 ... 125/ 65 ... 100	435 ... 475 475	6	200	–
TiAlN	-60 ... -150	$8 \times 10^{-3} \ldots 1.5 \times 10^{-2}$	85 ... 125/ 65 ... 115	430 ... 450	6	200	–
AlTiN	-90 ... -150	$4 \times 10^{-3} \ldots 1.2 \times 10^{-2}$	60 ... 125/ 52 ... 130		6	150 ... 200	–

capture and basic measurement functions were used to observe and evaluate the type and length of cracks. The evaluation of cyclic indentation experiments results of different coated systems was based on the following: the qualitative evaluation criteria of the cracking (0 ... VI) from crack formation, propagation to delamination of the coating was considered (Table 4).

COMPARATIVE ADHESION TESTING

The adhesion test on the Zwick/ZHR 8150 Rockwell hardness tester at an indentation load of 1471 N (150 kgf) was performed to assess the quality of the coatings. The test procedure followed the VDI 3198 (1992) standard [15].

RESULTS AND DISCUSSION

ADHESION TESTING

The results of the indentation test are presented by micrographs in Fig. 3. The micrographs of higher magnification are placed aside the main figures to indicate and specify coating cracking. The type and the volume of a failure zone indicate to film adhesion and its brittleness which correspond to the microstructure and the mechanical properties of the coatings. Coatings of higher hardness and lower Young's modulus (higher E/H ratio) withstand the load without nucleation of long radial and conical cracks (TiN and TiCN). However, considerable amount of long radial cracks of 10 ... 50 μm were generated, causing the exfoliation of coating layers that is a typical behaviour of TiN and TiCN coatings under loading [1]. The longest radial cracks are indicated in the TiN coating and numerous enfolds and larger in size exfoliations of the coating layer are observed (Fig. 3 (a)). It is obvious that radial cracks predispose that kind of coating failure. The same features are seen in the case of TiAlN coating with only difference - the conical cracks are also present (Fig. 3 (c)). It seems that short radial cracks accelerate chipping on the bordering area of coating-indenter contact. Emerged chips tend to make connections with the closest on the sides forming the ring or conical crack. The structural defects presented on the surface, such as pores and non-metallic inclusions, simplify this action.

Finally, the most drastically fractured case - nACo® coating (Fig. 3 (e)). The worst performance of this coating was indicated by the numerous short radial and closed conical cracks. First, the very brittle structure collapses around the indenter and then starts to take up (absorb) fracture energy by the formation of radial cracks. Eventually those are blunted by the perpendicularly formed conical

Table 4: *Crack types and crack evaluation criteria.*

Criteria	**0**	**I**	**II**	**III**	**IV**	**V**	**VI**
Crack type	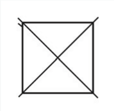	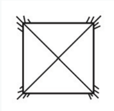	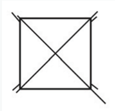	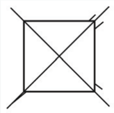	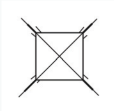	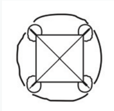	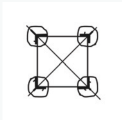
Crack type description	Very weak secondary radial cracks, which emanate from the edge and around the corners of the imprint.	Weak secondary radial cracks.	Medium secondary radial cracks and weak radial cracks - beginning of radial cracks formation.	Medium secondary radial cracks and medium radial cracks-propagation of weak radial cracks.	Medium secondary radial cracks and strong radial cracks.	Medium radial cracks, delamination of coating in the corners of the contact impression and cone (ring) cracks at the periphery of the imprint.	Strong radial cracks and delamination of the coating around the corners of the indent impression.

cracks and are not reaching the last "ring".

Among all the tested coatings, the TiCN seems to be most endurable. The mixed failure modes are characteristic of the studied coated system. Most widely presented are cohesive (chipping caused by the normal component of a stress tensor) and the delamination with buckling and fracture mode (decohesion of a coating with the formation of microcracks, caused by a combination of shear and normal stresses).

COATED SYSTEM BEHAVIOUR UNDER CYCLIC LOADING

The results of cyclic indentation are given in Table 5. After the first indentation cycle, mostly contact region model of coating deformation was presented due to the high indenting load of 500 N applied. With TiCN, no cracks at all or weak secondary radial cracks were observed in the corners of the impression (Fig. 6 (a)).

To estimate the cracking resistance of the coated system, a quantitative analysis of the samples was performed. The lengths of radial cracks from the impression corner were measured and presented on graphs (Fig. 4, 5) versus the number of indentation cycles. The error bars show the standard deviation of 2.3 μm.

Similarly to the single loading of the adhesion test, TiCN coating on both substrates had the best cracking resistance at all cycle values (Fig. 4). TiCN on Vanadis 6 showed radial cracks with a length of 20 μm and crack evaluation criteria II (Fig. 4 (a), Fig. 6 (a)). On the contrary, nACo® on both substrates had the lowest cracking resistance (Fig. 7 (c)). The cracking of this coating differed from others with the formation of cone cracks around the

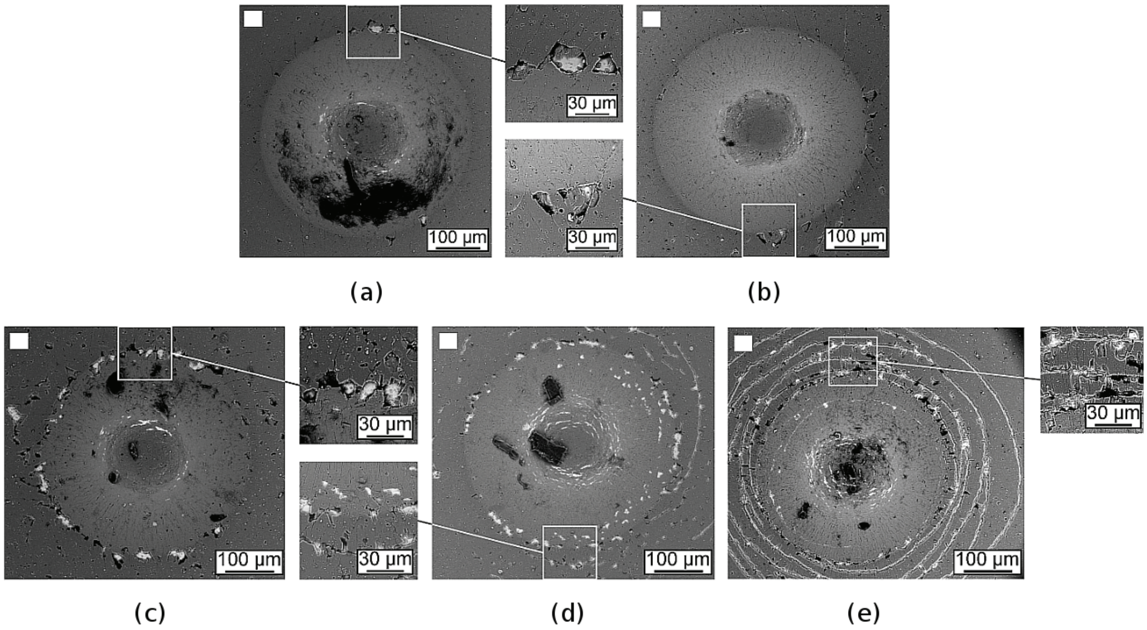

Fig. 3: *SEM micrographs of the adhesion test of coatings: (a) TiN; (b) TiCN; (c) TiAlN; (d) AlTiN and (e) nACo®.*

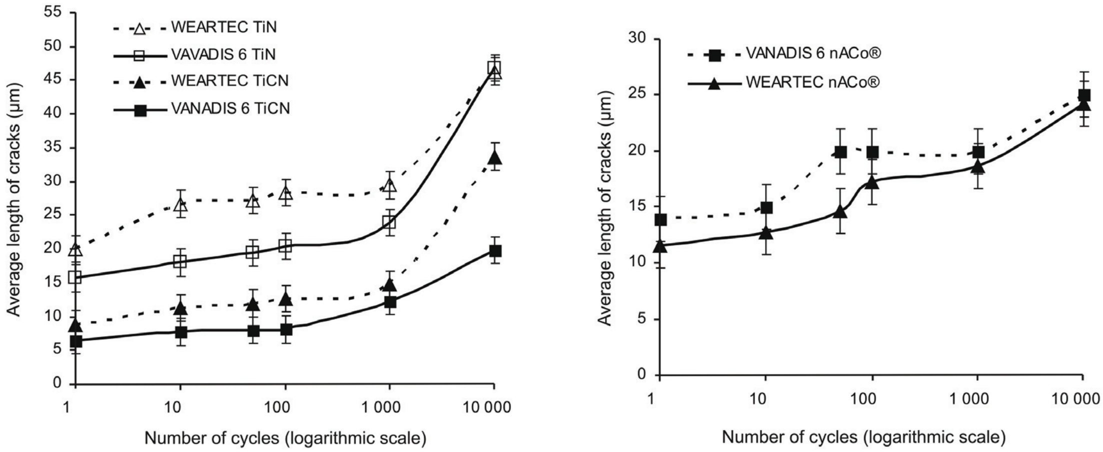

Fig. 4: *An average length of radial cracks measured from the indent impression corners depending on the number of indentation cycles, substrate material and coating combinations: (a) TiN and TiCN; (b) nACo on Weartec*^{TM} *and Vanadis 6 substrates.*

impression, in addition to radial cracks and delamination of the coating at indent impression corners validating the results of the adhesion test (Fig. 3 (e)).

The facts above allowed a hypothesis to be made that the crack type and cracking resistance of a cyclic loaded coated system is dependant on the coating E/H ratio. Radial cracking without delamination was observed in coatings with the highest E/H ratio (TiCN and TiN) and the lowest values

Table 5: *Observed crack types analysis.*

Coating / Substrate \ Observed crack types analysis	1	10	50	100	1000	10000
TiN / Weartec™	I	I	I	I, II	II	**IV**
TiN / Vanadis 6	I	I	I	I	II	**IV**
TiCN / Weartec™	0, I	0, I	0, I	I	I	**III**
TiCN / Vanadis 6	0	0	0	0, I	0, I	**II**
nACo® / Weartec™	I	I, II Starting delamination	II Starting delamination	II Starting delamination	V Cone crack	**V** Cone crack
nACo® / Vanadis 6	O	I Starting delamination	V Cone crack	V Cone crack	V Cone crack	**V** Cone crack
TiAlN / Weartec™	0, I	I	I	I, II	II, III	**VI**
AlTiN / Weartec™	I	I	I	I	II	**VI**

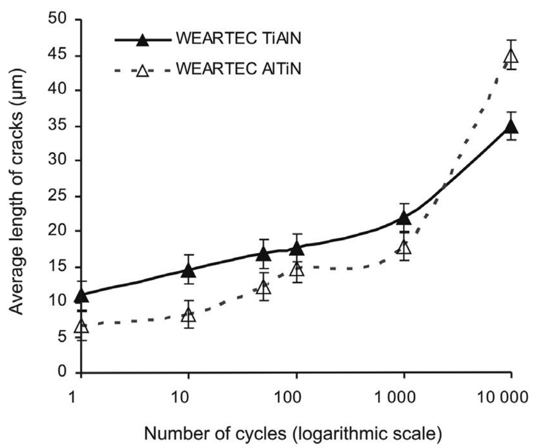

Fig. 5: *An average length of radial cracks measured from the indent impression corner depending on the number of indentation cycles of TiAlN and AlTiN on Weartec™ substrate.*

of E/H (nACo®) showed cone cracking and delamination. The dependence between radial cracking sequence and E/H ratio values was described in the form of a diagram (Fig. 8). Each curve on the diagram is associated with a certain number of indentation cycles. According to the diagram curves, TiAlN has medium and AlTiN strong radial cracks after 10 000 cycles. Both coatings showed

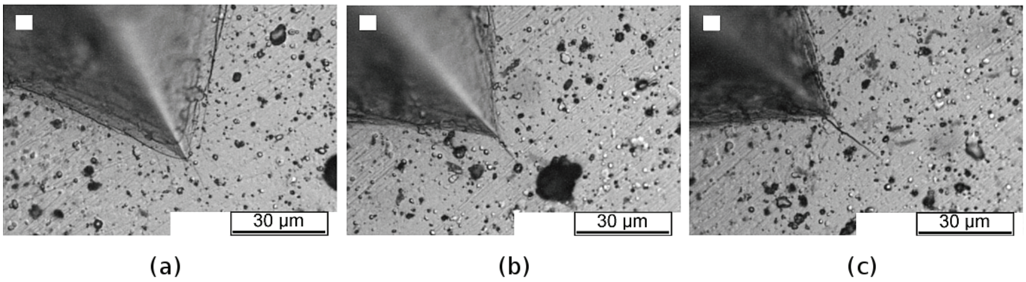

Fig. 6: *Impression corner of TiCN on Vanadis 6 substrate with the appearance of 0 criteria after: (a) 1 cycle. I criteria after: (b) 1000 cycles. II criteria after: (c) 10 000 cycles.*

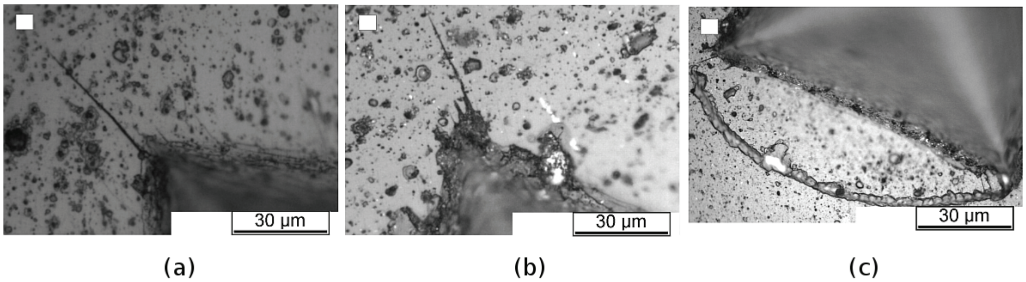

Fig. 7: *Impression corner of coatings on Weartec™ after 10 000 cycles with the appearance of IV criteria: (a) TiN; VI criteria: (b) AlTiN; V criteria: (c) nACo®.*

delamination of the coating around the corners of the impression. TiAlN was less damaged and it had higher E/H ratio than AlTiN (Fig. 7 (b)). In addition, cyclic indentation test revealed that multilayer coatings are preferable over monolayer TiN coating with one of the lowest cracking resistance and the formation of strong radial cracks with the length of about 47 μm despite high E/H ratio of TiN (Fig. 7 (a)).

Despite the lowest length of the radial cracks, as shown in the diagram (Fig. 8), nACo®coating on Weartec™ had the worst performance. The appearance of the shortest radial cracks can be explained by the formation of additional cone cracks after 1 000 and 10 000 indentation cycles what hamper the propagation of the radial cracks.

The "quasi-plastic" damage mode prevailed as the Vickers diamond pyramid was used in the indentation test. In contrast to spherical indenters, a sharp indenter penetrates easily into the coating surface and cone cracking formation is suppressed by the radial cracks nucleation. Radial cracks become the dominant mode of indentation fracture and lead to accelerated cracking resistance degradation of the coating. Fracture analysis revealed that apart from other coatings, in nACo® the "brittle" damage mode occurred with the formation of cone cracks, driven by tensile stresses in addition to "quasi-plastic". On the other hand, the obscured subsurface damage and the formation of radial cracks could be found below cone cracks.

The best cracking resistance of TiCN can be also explained by good adhesion due to the presence of the carbides in both substrates. Crystallographic similarity of the substrate and the coating seem to have an effect, ensuring strong bonding between them. The observations of both substrates coated with TiCN expose the advantages of PM steel Vanadis 6 over Weartec™, as it has higher Young's module. It is assumed that Vanadis 6 works like a spring under the coating, allowing it to bend and deform (fracture) according to the contact region wear model described above. In addition, Vanadis 6 smaller carbide size and uniform carbides

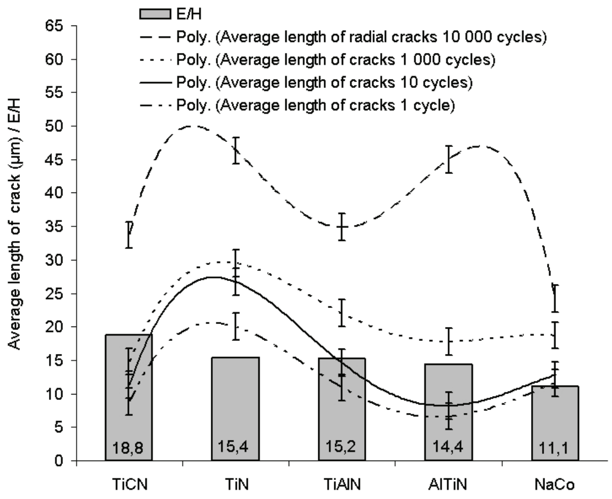

Fig. 8: *The effect of the E/H ratio on the radial crack propagation (coatings on Weartec™).*

distribution hampers the formation and propagation of cracks and delamination of the coating. However, Vanadis 6 as a substrate for TiN and nACo® did not show benefits over Weartec™.

CONCLUSIONS

Indentation cyclic tests of coated tool steels were carried out and the following conclusions can be drawn:

1. The increase of the number of the indentation cycles leads to the radial crack growth. It is obvious that cracking resistance and crack type is dependant on the Young's module/Hardness ratio values (E/H ratio) of the coating. Specifically, TiCN coating proved to have the best indentation cracking resistance for both substrate materials, as it had the highest E/H ratio value. Additionally, TiCN on Vanadis 6 showed less damage after 10 000 indentation cycles with (II) evaluation criteria of cracking resistance. Vanadis 6 steel has higher Young's module value and the finest microstructure also. Thus, the same conclusion can be drawn for substrate materials - their indentation cracking resistance is also dependent on the E/H ratio as well as its microstructure, carbides size and distribution.

2. Experiments revealed that the "quasi-plastic" damage mode, with the formation of radial cracks prevail in the indentation cycling testing and is typical of high E/H values of coatings. "Brittle" damage with the formation of cone cracks is characteristic of the cyclic loaded coatings with the lowest E/H ratio values.

3. Multilayer coatings had higher fatigue resistance than monolayer coating despite higher E/H ratio.

ACKNOWLEDGEMENT

Authors want to express their appreciation to the Estonian Ministry of Education and Research under project SF0140091s08 and the Estonian Science Foundation (Grants No. 7227, 7442 and 7889) for supporting the research.

REFERENCES

[1] Bouzakis K.-D., Siganos A., Leyendecker T., Erkens G., Thin hard coatings fracture propagation during the impact test, Thin Solid Films, vol. 460, 2004, p. 181–189.

[2] Chiang S.S., Marshall D.B., Evans A.G., The response of solids to elastic/plastic indentation, I. Stresses and residual stresses, J. Appl. Phys., vol. 53, 1982, p. 298–311.

[3] Chiang S.S., Marshall D.B., Evans A.G., The response of solids to elastic/plastic indenta-

tion, II. Fracture initiation, J. Appl. Phys., vol. 53, 1982, p. 312–317.

[4] Cook R.F., Pharr G.M., Direct observation and analysis of indentation cracking in glasses and ceramics, J. Am. Ceram. Soc., vol. 73, 1990, p. 787–817.

[5] Fouvry S., Liskiewicz T., Paulin C., A global-local wear approach to quantify the contact endurance under reciprocating-fretting sliding conditions, Wear, vol. 263, 2007, p. 518–531.

[6] Guiberteau F., Padture N.P., Cai H., Lawn B.R., Simple cyclic Hertzian test for measuring damage accumulation in polycrystalline ceramics, Philos. Mag. A, vol. 68, 1993, p. 1003–1016.

[7] Holmberg K., Ronkainen H., Laukkanen A., Wallin K., Hogmark S., Jacobson S., Wiklund U., Souza R.M., Ståhle P., Residual stresses in TiN, DLC and MoS2 coated surfaces with regard to their tribological fracture behaviour, 13th Nordic Symposium on Tribology NORDTRIB 2008, Tampere, Finland, 2008, 37 p.

[8] Kim D.K., Jung Y.-G., Peterson I.M., Lawn B.R., Cyclic contact fatigue of intrinsically brittle ceramics in contact with spheres, Acta Mater., vol. 47, 1999, p. 4711–4725.

[9] Lankford J., Davidson D.L., The crack initiation threshold in ceramic materials subject to elastic/plastic indentation, J. Mater. Sci., vol. 14, 1979, p. 1662–1668.

[10] Palmqvist S., The work for the formation of a crack during Vickers indentation as a measure of the toughness of hard metals (in Ger.), Arch. Eisenhuttenwes., vol. 33, 1962, p. 629–34.

[11] Richter J., Application of Vickers indentation for assessment of PVD TiN coated new nonledeburitic high-speed steels, Surf. Coat. Tech., vol. 162, 2003, p. 119–130.

[12] Sglavo V.M., Green D.J., Indentation determination of fatigue limits in silicate glasses, J.Am. Ceram. Soc., vol. 82, 1999, p. 1269–74.

[13] Shetty D.K., Wright I.G., Mincer P.N., Clauer A.H., Indentation fracture of WC-Co cermets = Rupture par indentation de cermets WC-Co, J. Mater. Sci., vol. 20, 1985, p. 1873–1882.

[14] Tarrés E., Ramirez G., Gaillard Y., Jimnez-Piqu E., Llanes L., Contact fatigue behavior of PVD-coated hardmetals, Int. J. Refract. Met. H. Mater., vol. 27, 2009, p. 323–331.

[15] VDI 3198:1992-08, Coating (CVD, PVD) of cold forging tools, VDI-Verlag, Dusseldorf, 1991.

[16] Zoestbergen E., De Hosson J.Th.M., Crack resistance of PVD coatings: Influence of surface treatment prior to deposition, Surf. Eng., vol. 18, 2002, p. 283–288.